Research Article
Limited Feedback Precoding for Massive MIMO

Xin Su, Jie Zeng, Jingyu Li, Liping Rong, Lili Liu, Xibin Xu, and Jing Wang

Tsinghua National Laboratory for Information Science and Technology, Tsinghua University, Beijing 100084, China

Correspondence should be addressed to Jie Zeng; zengjie@tsinghua.edu.cn

The large-scale array antenna system with numerous low-power antennas deployed at the base station, also known as massive multiple-input multiple-output (MIMO), can provide a plethora of advantages over the classical array antenna system. Precoding is important to exploit massive MIMO performance, and codebook design is crucial due to the limited feedback channel. In this paper, we propose a new avenue of codebook design based on a Kronecker-type approximation of the array correlation structure for the uniform rectangular antenna array, which is preferable for the antenna deployment of massive MIMO. Although the feedback overhead is quite limited, the codebook design can provide an effective solution to support multiple users in different scenarios. Simulation results demonstrate that our proposed codebook outperforms the previously known codebooks remarkably.

1. Introduction

High-rate data demand increases faster and faster with the new generation of devices (smart phones, tablets, netbooks, etc.). However, the huge increase in demand can be hardly met by current wireless systems. As is known to us, MIMO channels, created by deploying antenna arrays at the transmitter and receiver, promise high-capacity and high-quality wireless communication links by spatial multiplexing and diversity. Basically, the more antennas the transmitter or the receiver equipped with, the more degrees of freedom that the propagation channel can provide, and the higher data rate the system can offer. Therefore, there is significant effort within the community to research and develop massive MIMO technology, which is a hot topic nowadays [1].

For multiuser MIMO systems, we can utilize precoding to explore massive MIMO potentials. The essence of precoding techniques is to mitigate the interuser interference and to improve the effective received SNR. Herein, channel state information at the transmitter (CSIT) is an essential component when trying to maximize massive MIMO performance via precoding. In time division duplexing (TDD) system, channel reciprocity can be utilized for pilot training in the uplink to acquire the complete CSIT, but the pilot contamination and imperfect channel estimation based on uplink

pilots would lead to inaccuracy of the CSIT. In frequency division duplexing (FDD) system, the CSIT shall be acquired via the feedback channel, which is usually limited in practice. Hence, a finite set of precoding matrices, named codebook, known to both the receiver and the transmitter should be predesigned. The receiver selects the optimal precoding matrix from the codebook according to the channel state information (CSI) and reports the precoding matrix indicator (PMI) to the transmitter via the limited feedback channel [2]. With this mechanism, the system can obtain performance improvement by employing a well-designed codebook.

For traditional MIMO systems, several codebooks have been proposed, such as Kerdock codebook [3], codebooks based on vector quantization [4], Grassmannian packing [5], discrete Fourier transform (DFT) [6], and quadrature amplitude modulation [7]. Codebooks based on vector quantization have taken the channel distribution into account but have to be redesigned when the channel distribution changes. For uncorrelated channels, the Grassmannian is nearly the optimal codebook, but its construction requires numerical iterations, and with high storage requirement. The Kerdock codebook has simple systematic construction, significantly low storage, and selection computational requirements due to finite quaternary alphabet. However, the Grassmannian codebook and the Kerdock codebook are not optimized for
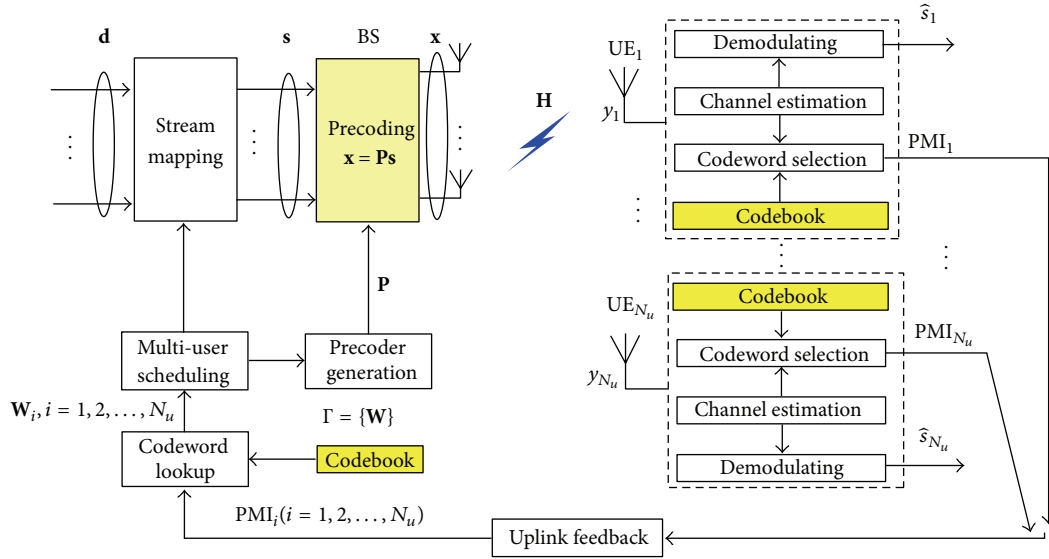
FIGURE 1: The feedback precoding model of the multiuser MIMO system.

correlated channels when closely spaced ($\lambda/2$) antenna arrays are employed. This case with the substantial correlation can be better reflected by DFT codebooks.

Traditionally, the uniform linear array (ULA) setup is adopted in a MIMO system. But for the consideration of constrained array aperture and aesthetic factor, the ULA setup is not suitable for massive MIMO. Besides, the linear array with antenna elements of identical gain patterns (e.g., isotropic elements) brings the problem of front-back ambiguity and is also unable to resolve signal paths in both azimuth and elevation [8]. For these reasons, the massive MIMO might employ two-dimensional array structures, such as the uniform rectangular array (URA). However, the current proposals of DFT codebooks fail to work well on the new antenna layout, since the codebook construction is aimed at the linear arrays, such as ULA. Thus, we need a new scheme to construct the codebook to better reflect the channel properties.

The rest of the paper is outlined as follows. In Section 2, we introduce the system model. In Section 3, we present the codebook designs including the novel codebook design for URA purpose. Then, we analyze the channel capacity and evaluate the performance of different codebooks in Section 4. Finally, we give some conclusions in Section 5.

2. System Model

In this paper, we focus on the downlink transmission of a massive MIMO system, that is, the base station (BS) with massive antennas as the transmitter and the user equipment (UE) as the receiver, and we adopt the multiuser MIMO transmission architecture with feedback precoding mechanism, as shown in Figure 1. The BS is equipped with N_t transmit antennas, and N_u UEs with N_r receive antennas, each is served by the BS in the cell; and the maximum number of spatial multiplexing UEs is K. In this paper, we assume that $N_r = 1$, $N_t \gg K$, and $K \geq 1$.

In order to report the CSI from the receiver to the transmitter via a limited feedback channel, we need to predesign a codebook. Given the codebook containing a list of codewords $\mathbf{W}_i$ at both the transmitter side and the receiver side, each of which reflects one state of the channel at a certain time, the receiver can only report an index within the codebook, called PMI, to the transmitter; then the transmitter obtains the PMI and queries the codebook to accomplish the precoding process.

For the codeword selection at the receiver, we can adopt the capacity selection criterion [5] which is to maximize the channel gain given the channel matrix $\widehat{\mathbf{H}}$ by traversing the whole codebook Γ:

$$\mathbf{W}_k^{\mathrm{opt}} = \mathbf{W}^\Gamma \left(\widehat{\mathbf{H}}_k\right) = \max_{\mathbf{W} \in \Gamma} \left\| \mathbf{W}\widehat{\mathbf{H}}_k \right\|_2^2. \tag{1}$$

For a multiuser MIMO system, we need to select K UEs to serve simultaneously from a larger number of UEs. Thus, a scheduling module is necessary to select proper UEs. All UEs shall report their own requested codewords $\mathbf{W}_i$; and then we can find out the UE set to schedule according to certain scheduling criteria. After determining the scheduled UEs, the transmitter starts the following data transmission procedure: firstly, multiplexing streams denoted by the vector $\mathbf{s}$ are selected from the user data stream $\mathbf{d}$ inputting in the system according to the multiuser scheduling module; secondly, the data is preprocessed by a precoder $\mathbf{P}$ which is formed by combining the UEs' requested codewords column by column, and we get the transmit signal $\mathbf{x}$:

$$\mathbf{x} = \mathbf{Ps}, \tag{2}$$

where $\mathbf{s} = [s_1, s_2, \ldots, s_K]$, $\mathbf{P} = [\mathbf{W}_{s(1)}, \mathbf{W}_{s(2)}, \ldots, \mathbf{W}_{s(K)}]$, and $\mathbf{W}_{s(i)}$ denotes the codeword for scheduled UE $s(i)$. For the sake of clarity without misunderstanding, we use $\mathbf{W}_i$ instead of $\mathbf{W}_{s(i)}$ in the following expressions.

After $\mathbf{x}$ passing the channel and being added the noise, we will get the received signal $\mathbf{y}$:

$$\mathbf{y} = \mathbf{H}\mathbf{x} + \mathbf{z} = \mathbf{H}\mathbf{P}\mathbf{s} + \mathbf{z}, \qquad (3)$$

where $\mathbf{H}$ denotes the channel matrix of size $(K \times N_t)$ with its entry H_{ij} denoting the complex channel response from the jth transmit antenna to the ith UE's receive antenna, and $\mathbf{z}$ is the additive white complex Gaussian noise (AWGN) vector with covariance matrix $\sigma^2 \mathbf{I}_K$. For UE k, the received signal y_k is

$$\begin{aligned} y_k &= \mathbf{H}_k \mathbf{x}_k + \sum_{i \neq k} \mathbf{H}_k \mathbf{x}_i + z_k, \\ &= \mathbf{H}_k \mathbf{W}_k s_k + \sum_{i \neq k} \mathbf{H}_k \mathbf{W}_i s_i + z_k. \end{aligned} \qquad (4)$$

After UE k obtains the estimated channel matrix $\widehat{\mathbf{H}}_k$ through the channel estimation, it demodulates the received signal y_k:

$$\widehat{s}_k = d_k y_k. \qquad (5)$$

If the interference is unaware to the receiver, which means that it is treated as part of the noise, the matched filter (MF) is usually adopted:

$$d_k = \left(\widehat{\mathbf{H}}_k \mathbf{W}_k \right)^*. \qquad (6)$$

3. Codebook Design

The codebook design is a quantization problem, in which we should balance the accuracy and the overhead of bits. The Grassmannian codebook would offer the optimal solution for fully uncorrelated channels [5], but it is not practical for massive MIMO systems due to its difficulty of construction for higher-dimensional space. Kerdock can be easily extended to massive transmit antennas due to its systematic construction and low codeword selection complexity. However, like the Grassmannian codebook, the Kerdock codebook is only suitable for uncorrelated channels. For high-correlated channels, a DFT codebook able to respond the channel correlation provides a good fit. Since the channels are likely to be highly correlated due to the closely spaced arrays probably utilized by massive MIMO, we focus on the DFT codebook and its extension for massive MIMO with the URA deployment.

3.1. The Traditional DFT Codebook. Closely spaced arrays, including both crosspolarized and copolarized ones, imply certain spatial correlation structures which may be utilized to compress the channel into an effective channel of lower dimensionality. With such setup, the channel is spatially correlated, and the spatial covariance matrix can be approximated using its eigenvectors with the closely spaced ($\lambda/2$) array. The linear DFT codebook design targets at the linear closely spaced array, which has two separate parts representing long-term and short-term channel states, respectively [6, 9]. The first codeword $\mathbf{W}^1$ in the long-term feedback part consists of multiple beams such that the beams cover the full

signal space over the wideband with closely-spaced arrays, hence capturing the correlation properties of the channel. The second codeword $\mathbf{W}^2$ in the short-term feedback part combines the beams to capture short-term variations. The final precoder $\mathbf{W}$ is given by

$$\mathbf{W} = \mathbf{W}^1 \mathbf{W}^2. \qquad (7)$$

This is the DFT codebook design for the ULA [10]. It is noted that the design essentially comes from the concept of the adaptive codebook [11]. Under the assumption that the channel correlation is both known by the transmitter with multiple antennas and the receiver with single antenna, the precoder can be computed by

$$\mathbf{W} = \mathbf{R}^{1/2} \mathbf{V}, \qquad (8)$$

where $\mathbf{R}$ is the spatial covariance matrix of the channel $\mathbf{H}$, that is, $\mathbf{R} = E[\mathbf{H}^H \mathbf{H}]$, and $\mathbf{V}$ is a $N_t \times 1$ codeword of a uniform codebook. Adaptive codebook is well known to provide good performance in correlated channels, especially for multiuser MIMO. In practical application, a double codebook is utilized to minimize the feedback overhead. The transmitter and the receiver could share the knowledge of the matrix $\mathbf{R}$ through the feedback of first codeword $\mathbf{W}^1$. This feedback overhead is low even though the information of $\mathbf{R}$ is vast, since the feedback interval could be very long due to the stable channel correlation. Besides, the second codeword $\mathbf{W}^2 = \mathbf{V}$ is reported more frequently to represent the short-term variations. The precoder $\mathbf{W} = \mathbf{W}^1 \mathbf{W}^2$ can adapt to the angular spread of the channel by covering the instantaneous subspace over the entire band.

For the copolarized arrays of closely spaced ($\lambda/2$) antenna elements, the codeword $\mathbf{W}^1$ in the long-term feedback codebook is expressed as

$$\mathbf{W}^1(g) = \mathbf{D}(g), \qquad (9)$$

where $\mathbf{D}(g)$ ($g = 0, 1, \ldots, G-1$) are DFT rotation matrices with the size $N \times M$, G is the total number of DFT matrices, and each element can be expressed as

$$[\mathbf{D}(g)]_{n,m} = \frac{1}{\sqrt{N}} \exp\left(j \frac{2\pi}{M} n \left(m + \frac{g}{G} \right) \right), \qquad (10)$$

where $n = 0, 1, \ldots, N-1$ and $m = 0, 1, \ldots, M-1$. Here, we have $N = N_t$ and $G = 2^B/M$, where B is the codebook size, that is, the feedback overhead (in bits).

While the first codeword $\mathbf{W}^1$ describes the correlation property of the channel, the second codeword $\mathbf{W}^2$ consists of beam selection vectors. Since the size and the energy of the UEs are usually limited, frequently only one antenna is employed in practical. As a result, rank-1 channels are essential for current multiuser MIMO. For the rank-1 channel, it has the form

$$\mathbf{W}^2(i_2) = \mathbf{v}_{i_2}, \qquad (11)$$

where $\mathbf{v}_k$ is a $M \times 1$ selection vector that has 1 on the kth row and 0 elsewhere and i_2 indicates the index of $\mathbf{W}^2$ in the second part of the codebook.

Above are the constructions for the linear closely spaced antenna elements. Under such scenarios with the substantially correlated channels, the DFT-based codebook is able to respond the correlation. However, for two-dimensional antenna arrays, the long-term statistical properties of the channel cannot be directly reflected by DFT vectors, since every DFT vector can only represent the beams emitted by the linear closely spaced antenna elements. Hence, we need to extend the DFT codebook to adapt to two-dimensional array structures, like the URA.

3.2. The Proposed Codebook

3.2.1. Kronecker-Type Approximation of Correlation. In this paper, we consider a URA lying on the XY plane with x-axis parallel to one edge of the URA and y-axis parallel to the other vertical edge, as shown in Figure 2 taking 64 copolarized antennas as an example.

We assume that the correlation between the antenna elements along x does not depend on the antenna elements along y and its correlation matrix is described as matrix $\mathbf{R}_x$; the correlation along y does not depend on the antenna elements along x and its correlation matrix is described as matrix $\mathbf{R}_y$. Thus, we have the following Kronecker-type approximation for the URA correlation matrix [12]:

$$\mathbf{R} = \mathbf{R}_x \otimes \mathbf{R}_y, \tag{12}$$

where $\otimes$ denotes the Kronecker product.

Formula (12) indicates that the URA correlation matrix $\mathbf{R}$ is the Kronecker product of two ULA correlation matrices $\mathbf{R}_x$ and $\mathbf{R}_y$. This approximation model is reasonably accurate, allowing the well-developed theory of Toeplitz matrices for the analysis of multidimensional antenna arrays. In the following, we take the Kronecker-type approximation model as the theoretical basis of the first codeword construction.

3.2.2. Codebook Construction

Theorem 1. *If $\mathbf{X}$ and $\mathbf{Y}$ are diagonalizable square matrices, then*

$$(\mathbf{X} \otimes \mathbf{Y})^{1/2} = \mathbf{X}^{1/2} \otimes \mathbf{Y}^{1/2}. \tag{13}$$

Proof. Firstly, we prove that $(\mathbf{D}_x \otimes \mathbf{D}_y)^{1/2} = \mathbf{D}_x^{1/2} \otimes \mathbf{D}_y^{1/2}$ for diagonal matrices $\mathbf{D}_x$ and $\mathbf{D}_y$.

Suppose that $\mathbf{D}_x = \mathrm{diag}(\lambda_1, \lambda_2, \ldots, \lambda_n), \mathbf{D}_y = \mathrm{diag}(\mu_1, \mu_2, \ldots, \mu_n)$, then

$$\mathbf{D}_x^{1/2} \otimes \mathbf{D}_y^{1/2}$$
$$= \mathrm{diag}\left(\lambda_1^{1/2}, \lambda_2^{1/2}, \ldots, \lambda_n^{1/2}\right)$$
$$\otimes \mathrm{diag}\left(\mu_1^{1/2}, \mu_2^{1/2}, \ldots, \mu_n^{1/2}\right)$$
$$= \mathrm{diag}\left(\left(\lambda_1\mu_1\right)^{1/2}, \left(\lambda_2\mu_1\right)^{1/2}, \ldots, \left(\lambda_n\mu_1\right)^{1/2},\right.$$
$$\left.\left(\lambda_1\mu_2\right)^{1/2}, \ldots, \left(\lambda_n\mu_2\right)^{1/2}, \ldots, \left(\lambda_n\mu_n\right)^{1/2}\right)$$

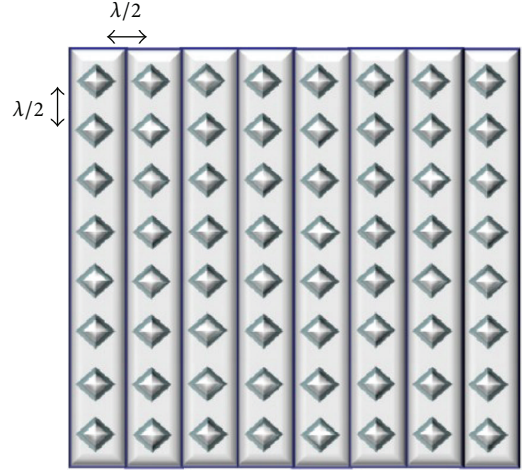
Figure 2: An example of the URA deployment for 64 antennas.

$$= \left(\mathrm{diag}\left(\lambda_1\mu_1, \lambda_2\mu_1, \ldots, \lambda_n\mu_1, \lambda_1\mu_2,\right.\right.$$
$$\left.\left.\lambda_2\mu_2, \ldots, \lambda_n\mu_2, \ldots, \lambda_n\mu_n\right)\right)^{1/2}$$
$$= \left(\mathbf{D}_x \otimes \mathbf{D}_y\right)^{1/2}. \tag{14}$$

An $n \times n$ matrix $\mathbf{A}$ is diagonalizable if there is a matrix $\mathbf{V}$ and a diagonal matrix $\mathbf{D}$ such that $\mathbf{A} = \mathbf{V}\mathbf{D}\mathbf{V}^{-1}$. In this case, the square root of $\mathbf{A}$ is $\mathbf{R} = \mathbf{V}\mathbf{D}^{1/2}\mathbf{V}^{-1}$. With this rule, we can prove the equation for any diagonalizable square matrices $\mathbf{X}$ and $\mathbf{Y}$.

Suppose $\mathbf{X} = \mathbf{V}_x\mathbf{D}_x\mathbf{V}_x^{-1}$ and $\mathbf{Y} = \mathbf{V}_y\mathbf{D}_y\mathbf{V}_y^{-1}$, then

$$\mathbf{X}^{1/2} \otimes \mathbf{Y}^{1/2} = \left(\mathbf{V}_x\mathbf{D}_x^{1/2}\mathbf{V}_x^{-1}\right) \otimes \left(\mathbf{V}_y\mathbf{D}_y^{1/2}\mathbf{V}_y^{-1}\right)$$
$$= \left(\mathbf{V}_x \otimes \mathbf{V}_y\right)\left(\mathbf{D}_x^{1/2} \otimes \mathbf{D}_y^{1/2}\right)\left(\mathbf{V}_x^{-1} \otimes \mathbf{V}_y^{-1}\right) \tag{15}$$
$$= \left(\mathbf{V}_x \otimes \mathbf{V}_y\right)\left(\mathbf{D}_x^{1/2} \otimes \mathbf{D}_y^{1/2}\right)\left(\mathbf{V}_x \otimes \mathbf{V}_y\right)^{-1},$$

$$\mathbf{X} \otimes \mathbf{Y} = \left(\mathbf{V}_x\mathbf{D}_x\mathbf{V}_x^{-1}\right) \otimes \left(\mathbf{V}_y\mathbf{D}_y\mathbf{V}_y^{-1}\right)$$
$$= \left(\mathbf{V}_x \otimes \mathbf{V}_y\right)\left(\mathbf{D}_x \otimes \mathbf{D}_y\right)\left(\mathbf{V}_x^{-1} \otimes \mathbf{V}_y^{-1}\right) \tag{16}$$
$$= \left(\mathbf{V}_x \otimes \mathbf{V}_y\right)\left(\mathbf{D}_x \otimes \mathbf{D}_y\right)\left(\mathbf{V}_x \otimes \mathbf{V}_y\right)^{-1},$$

$$(\mathbf{X} \otimes \mathbf{Y})^{1/2} = \left(\mathbf{V}_x \otimes \mathbf{V}_y\right)\left(\mathbf{D}_x \otimes \mathbf{D}_y\right)^{1/2}\left(\mathbf{V}_x \otimes \mathbf{V}_y\right)^{-1}$$
$$= \left(\mathbf{V}_x \otimes \mathbf{V}_y\right)\left(\mathbf{D}_x^{1/2} \otimes \mathbf{D}_y^{1/2}\right)\left(\mathbf{V}_x \otimes \mathbf{V}_y\right)^{-1}. \tag{17}$$

The formulae (15) and (16) utilize the Kronecker product properties including mixed-product property and the inverse property [13].

Thus, $(\mathbf{X} \otimes \mathbf{Y})^{1/2} = \mathbf{X}^{1/2} \otimes \mathbf{Y}^{1/2}$. $\square$

Since first codeword $\mathbf{W}^1$ reflects the channel correlation, we shall design it to satisfy

$$\mathbf{W}^1 = \mathbf{R}^{1/2}. \tag{18}$$

With formula (12) and Theorem 1, we have

$$\mathbf{W}^1 = \mathbf{R}^{1/2} = \left(\mathbf{R}_x \otimes \mathbf{R}_y \right)^{1/2} = \mathbf{R}_x^{1/2} \otimes \mathbf{R}_y^{1/2}. \tag{19}$$

Hence, assuming $\mathbf{D}_x(g_x)$ and $\mathbf{D}_y(g_y)$ are two DFT rotation matrices designed for two orthogonal ULAs, we can construct $\mathbf{W}^1$ for the URA with the Kronecker product of the two matrices:

$$\mathbf{W}^1(i_1) = \mathbf{D}_x(g_x) \otimes \mathbf{D}_y(g_y),$$

$$\left[\mathbf{D}_x(g_x) \right]_{n,m} = \frac{1}{\sqrt{N_x}} \exp\left(j \frac{2\pi}{M_x} n \left(m + \frac{g_x}{G_x} \right) \right),$$

$$\left[\mathbf{D}_y(g_y) \right]_{n,m} = \frac{1}{\sqrt{N_y}} \exp\left(j \frac{2\pi}{M_y} n \left(m + \frac{g_y}{G_y} \right) \right), \tag{20}$$

where i_1 indicates the index of $\mathbf{W}^1$ in the long-term feedback codebook, and g_x and g_y denote the indexes of the rotation DFT matrices for two directions, respectively. We have the following:

$$i_1 = G_y g_x + g_y, \quad g_x = 0, 1, \ldots, G_x - 1,$$

$$g_y = 0, 1, \ldots, G_y - 1. \tag{21}$$

Take the URA-64 in Figure 2 as an example: we have $N_x = 8$, $N_y = 8$, and $\mathbf{W}^1$ with the size of $64 \times M_x M_y$.

The construction of the $M_x M_y \times 1 \mathbf{W}^2$ is the same as the one for the ULA purpose (see formula (11)).

4. Evaluation

4.1. Channel Coverage. In this paper, for the rank-1 codebook which means that the number of spatial streams for a user is 1, we define the channel coverage as the gain using the codebook relative to the gain obtained by MF precoding with perfect CSIT:

$$C = E_{\mathbf{H}} \left[\frac{\left| \mathbf{H} \mathbf{W}^\Gamma(\mathbf{H}) \right|^2}{\left| \mathbf{H} \mathbf{W}^{\text{opt}}(\mathbf{H}) \right|^2} \right], \tag{22}$$

where $\mathbf{W}^\Gamma(\mathbf{H})$ indicates the codeword selected from the codebook Γ and $\mathbf{W}^{\text{opt}}(\mathbf{H}) = \mathbf{H}^*/\|\mathbf{H}\|_2$ is the optimal precoding matrix with perfect CSIT. The channel coverage can be used as a metric for the quality of a quantized codebook.

4.2. Sum Rate. In order to evaluate the precoding performance in a multiuser MIMO system, we can use the sum rate metric. For the downlink of the system, the optimal sum rate can be achieved by the interference presubtraction coding technique called dirty-paper coding (DPC), as long as the transmitter has perfect side information about the additive interference at the receiver [14]. The optimal DPC sum rate for the multiuser case is given as follows [15]:

$$R_{\text{DPC}} = E_{\mathbf{H}} \left[\max_{\boldsymbol{\Lambda}} \left(\log_2 \det \left(\mathbf{I}_{N_t} + \gamma \mathbf{H}^H \boldsymbol{\Lambda} \mathbf{H} \right) \right) \right], \tag{23}$$
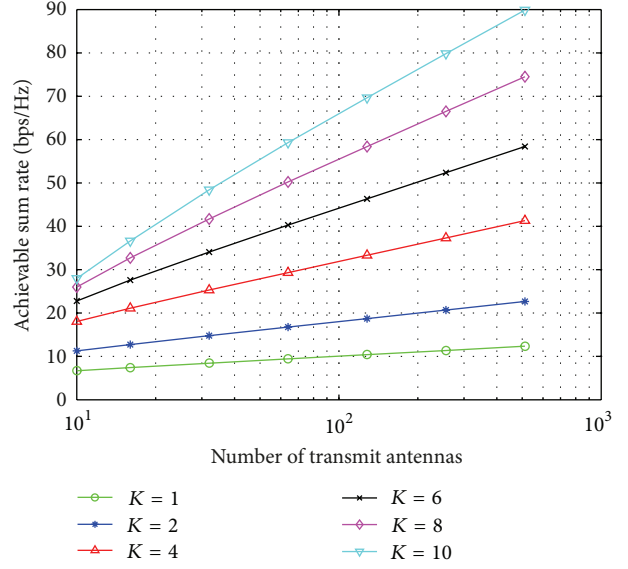
FIGURE 3: Optimal sum rate curves of different K values for $\gamma = 10$ dB.

where $\boldsymbol{\Lambda}$ is a $K \times K$ diagonal matrix for power allocation with factor λ_i on its main diagonal and $\sum \lambda_i = 1$.

Figure 3 depicts the optimal sum rate curves achieved by DPC for multiuser MIMO with K scheduled UEs equipped single-receive antenna under 10 dB SNR setting. Since the curves for different NLOS scenarios defined by [16], including urban macrocell (UMa), urban microcell (UMi), and indoor hotspot (InH) of the URA deployment are very close, we only draw the curves for the UMa scenario in this figure. From the result, we can see that the optimal sum rate increases linearly with the increase of the logarithm of N_t that is, we need to double the number of antennas in order to improve the capacity by roughly K bps/Hz. However, for large numbers of transmit antennas, the signal processing complexity, scheduling algorithm complexity for numerous users, and the CSI feedback overhead are significantly high, which may overshadow the capacity gain.

While the optimal sum rate can be used as the upper bound for the limited feedback precoding, the achievable sum rate of the precoding system using a quantized codebook can be used as an important indicator of the quality of the codebook [17]. For the multiuser MIMO system, if the channel estimation is considered to be ideal (i.e., $\widehat{\mathbf{H}}_k = \mathbf{H}_k$), the power of each transmit antenna is uniform, and the MF receiver is adopted (as shown in formula (6)) the instantaneous achievable sum rate can be expressed as

$$R(\mathbf{H}) = \sum_{k=1}^{K} \log_2 \left(1 + \frac{\|\mathbf{H}_k \mathbf{W}_k\|_2^2}{K/\gamma + \sum_{i \neq k} \|\mathbf{H}_k \mathbf{W}_i\|_2^2} \right), \tag{24}$$

where K is the number of scheduled users, $\gamma = P_t/\sigma^2$ is the signal-to-noise ratio (SNR) with P_t as the total transmit

power, $\mathbf{H}_k$, the column vector of $\mathbf{H}$ denotes the channel matrix for UE k, and $\mathbf{W}_k$ is its requested codeword.

Derivation. The received signal for UE k can be expressed as

$$y_k = \mathbf{H}_k \mathbf{W}_k s_k + \sum_{i \neq k} \mathbf{H}_k \mathbf{W}_i s_i + z_k. \tag{25}$$

With formula (6), the demodulated signal can be written as

$$\begin{aligned}
\widehat{s}_k &= \left(\mathbf{H}_k \mathbf{W}_k\right)^* y_k = \left|\mathbf{H}_k \mathbf{W}_k\right|^2 s_k \\
&\quad + \left(\mathbf{H}_k \mathbf{W}_k\right)^* \sum_{i \neq k} \mathbf{H}_k \mathbf{W}_i s_i + \left(\mathbf{H}_k \mathbf{W}_k\right)^* z_k.
\end{aligned} \tag{26}$$

And the power of the demodulated signal is

$$\begin{aligned}
E\left[\widehat{s}_k^* \widehat{s}_k\right] &= \left|\mathbf{H}_k \mathbf{W}_k\right|^4 E\left[s_k^* s_k\right] + \left|\mathbf{H}_k \mathbf{W}_k\right|^2 E\left[z_k^* z_k\right] \\
&\quad + \sum_{i \neq k} \left|\left(\mathbf{H}_k \mathbf{W}_k\right)^* \mathbf{H}_k \mathbf{W}_i\right|^2 E\left[s_i^* s_i\right] \\
&= \left|\mathbf{H}_k \mathbf{W}_k\right|^2 \left(\frac{P_t}{K} \left|\mathbf{H}_k \mathbf{W}_k\right|^2 + \sigma^2 + \frac{P_t}{K} \sum_{i \neq k} \left\|\mathbf{H}_k \mathbf{W}_i\right\|_2^2 \right).
\end{aligned} \tag{27}$$

Noting that the first term is the power of the wanted signal while the second and the third ones denote the power of the noise and the interference, we can compute the SINR as follows:

$$\text{SINR} = \frac{\left(P_t/K\right) \left|\mathbf{H}_k \mathbf{W}_k\right|^2}{\sigma^2 + \left(P_t/K\right) \sum_{i \neq k} \left\|\mathbf{H}_k \mathbf{W}_i\right\|_2^2} = \frac{\left\|\mathbf{H}_k \mathbf{W}_k\right\|_2^2}{K/\gamma + \sum_{i \neq k} \left\|\mathbf{H}_k \mathbf{W}_i\right\|_2^2}. \tag{28}$$

Thus, we have the instantaneous achievable sum rate expression given by formula (24).

The ergodic achievable rate can be expressed as

$$R = E_{\mathbf{H}} \left(R\left(\mathbf{H}\right)\right). \tag{29}$$

In order to evaluate the codebooks with the achievable sum rate metric, we adopt the Monte-Carlo simulation method and take the arithmetic mean of the instantaneous values under different channel realizations as the output metric. The simulation flow is described by the pseudocode in Algorithm 1.

4.3. Results. Based on the evaluation metrics, we present some simulation results in this section. The Winner II channel model [18] can be used for the ULA deployment in the simulation. But it needs to be modified to support the URA deployment. Thus, we extend the model by associating elevation angles to paths generated by the original Winner II model and correlating elevation statistics with other large-scale fading parameters. Without loss of generality, we take the case of 64 transmit antennas as an example for the performance evaluation of different codebook designs under different scenarios. For the sake of clarity, the conventional

```
// L: the total number of channel realizations
// N_u: the total number of UEs
// K: the number of scheduled UEs
Initialization
for l = 1 : L
    generate the channel matrix H
    for u = 1 : N_u
        compute the requested codeword W_u
        report W_u to the BS
    end for
    scheduling: select K UEs from the N_u UEs
    form the precoder P
    compute the instantaneous rate R_l (formula (23))
end for
Compute the metric R̄ = (1/L) Σ_{l=1}^{L} R_l
output R̄
```

Algorithm 1: Simulation flow.

ULA DFT codebook and the proposed URA DFT codebook are termed as DFT-ULA and DFT-URA, respectively.

Table 1 gives the parameter configuration for the following simulations. As we are discussing the capability of codebooks to reflect the channel correlation, we focus on the design of the first codeword $\mathbf{W}^1$ for DFT codebooks; hence, we set $M = 1$, which means that the codebooks have only one second codeword; that is, $\mathbf{W}^2 = 1$.

4.3.1. Channel Coverage. With the fixed number of transmit antennas, the codebook can be enlarged in order to improve the quantization accuracy, but the feedback overhead would limit the codebook size and codeword selection complexity would become a significant bottleneck. Consequently, it is necessary for us to investigate the performance of codebooks with different feedback overhead limits. Figure 4 presents the channel coverage defined by formula (22) as a function of the feedback overhead (B) for the DFT-ULA, the DFT-URA, and the Kerdock codebook under different NLOS scenarios with the URA deployment. It is noted that the maximum number of codewords in the Kerdock codebook for 64-dimensional space is 4096, and thus, the curve ends at the point of 12-bit feedback overhead. From the curves, we can see that when the feedback overhead becomes larger than 10 bits, the improvement becomes insignificant. In conclusion, the 8~10 bits of feedback is adequate for 64 transmit antennas with the URA. This feedback overhead is close to that of LTE-Advanced Release 10 in which the 8-bit rank-1 codebook for eight crosspolarized antennas is utilized [19]. Besides, effective approaches [20] can be used to further reduce the feedback overhead.

4.3.2. Achievable Sum Rate. We have run the multiuser MIMO simulation described in Algorithm 1 with 10-bit feedback overhead (i.e., $B = 10$), and the results are shown in Figures 5 and 6.

Table 1: Simulation configuration.

Parameter	Value
Channel model	UMa NLOS; UMi NLOS; InH NLOS
BS antenna setup	URA, 64 copolarized antennas, and $\lambda/2$ spacing
UE antenna setup	Single antenna
System frequency (GHz)	2.1
Number of channel realizations	1000
Number of UEs	10
Scheduling criteria	Minimizing the codeword correlation coefficient
Number of DFT matrices	
DFT-ULA	$G = 2^B$
DFT-URA	$G_x = G_y = 2^{B/2}$
Size of DFT matrices	
DFT-ULA	$N = 64, \; M = 1$
DFT-URA	$N_x = N_y = 8, \; M_x = M_y = 1$
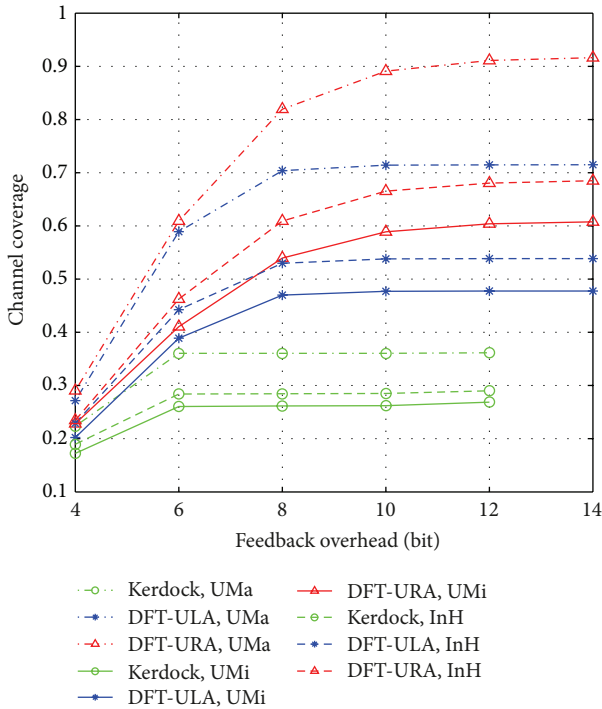
Figure 4: Channel coverage as a function of the feedback overhead.

Figure 5: Achievable sum rate as a function of K for $\gamma \to \infty$ and $\gamma = 10$ dB.

Figure 5 illustrates the curves as a function of the number of scheduled UEs (K) in the UMa scenario. From the curves, we can see that the DFT-URA outperforms the other codebooks for different number of UEs with $\gamma = 10$ dB. Figure 5 also shows the asymptotic curves as $\gamma \to \infty$, which measure the impact of the interuser interference. The gap between the DFT-URA and the DFT-ULA indicates that the DFT-URA can better mitigate the inter-user interference. Besides, in the capability of the inter-user interference suppression, the DFT-URA defeats the Kerdock when the number of scheduled UEs is relatively large ($K > 5$), since the DFT-URA is able
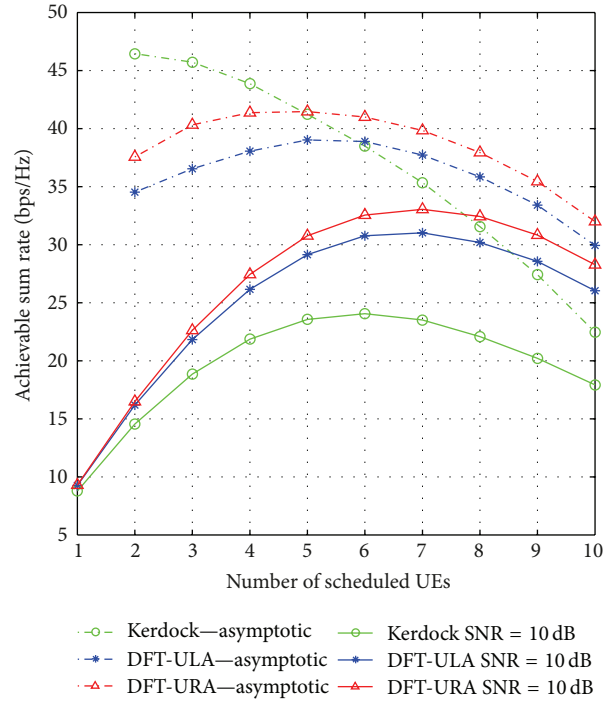
to provide more beams targeting at more UEs separated in different angular positions.

Figure 6 depicts the achievable sum rate of the Kerdock, the DFT-ULA, and the DFT-URA for four scheduled UEs ($K = 4$) as a function of SNR under the three scenarios; the theoretical curves drawn by formula (23) with perfect CSIT are presented as the upper bound. The results indicate that the DFT-URA designed to the URA deployment has remarkable performance gain compared to the DFT-ULA and especially the Kerdock codebook under different scenarios. It is because the design based on the Kronecker-type approximation of
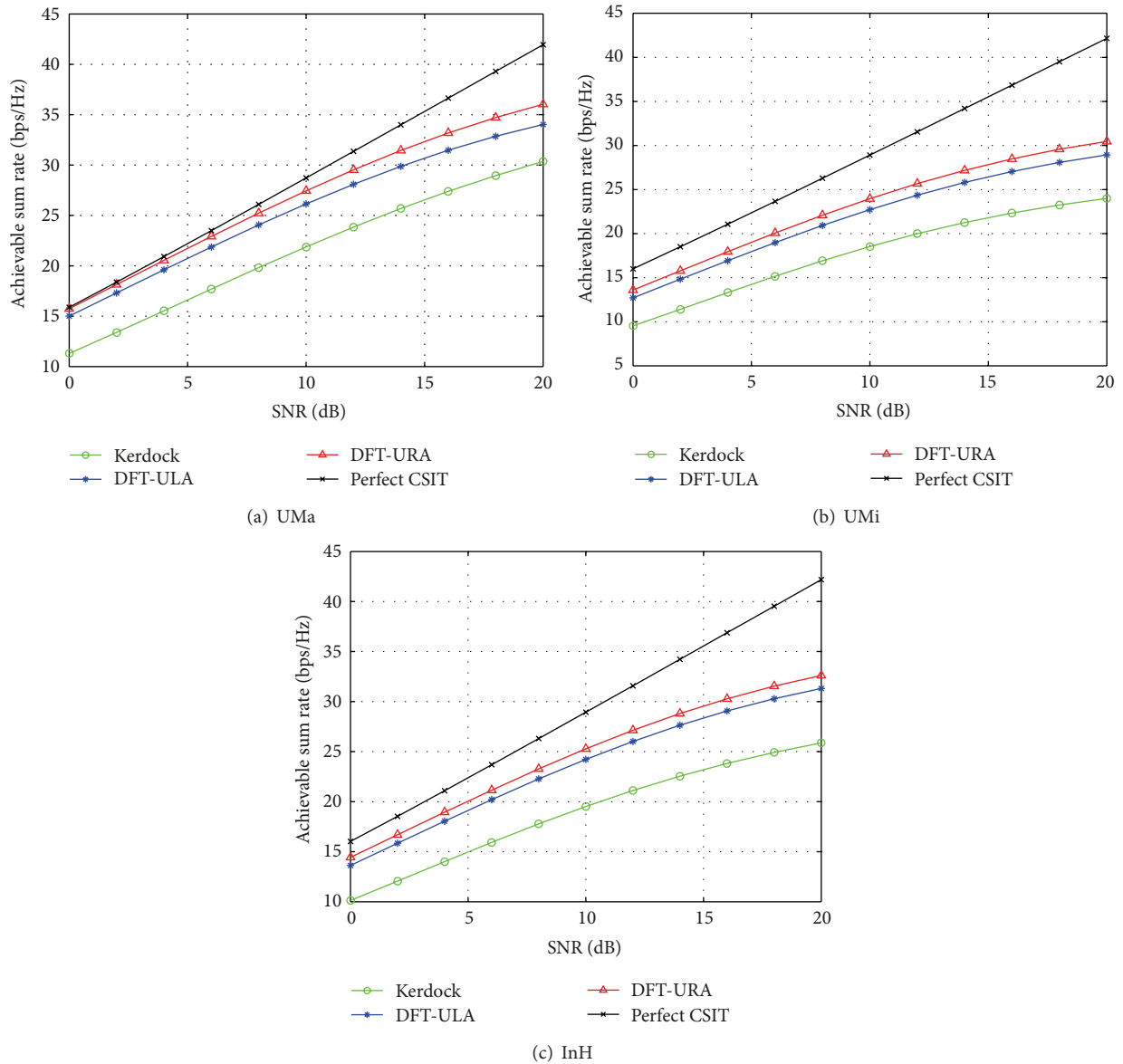
(a) UMa

(b) UMi

(c) InH

FIGURE 6: Achievable sum rate with $K = 4$. (a) Uma, (b) UMi, and (c) InH.

the array correlation structure better reflects the channel property with the URA, and thus physically leads to more accurate beams, making it suitable for multiuser MIMO in the case where UEs are separated spatially in angular domain. In addition, the performance in the UMa scenario is better than the other two scenarios, since this scenario has stronger channel correlation, making the DFT vectors better adapt to the channel.

5. Conclusion

In this paper, we discussed the limited feedback precoding techniques for the downlink of massive MIMO systems. On the theoretical basis of Kronecker-type approximation of the array correlation structure, we proposed a novel codebook

design for the URA deployment of the numerous closely spaced antennas, which would be probably adopted by massive MIMO. This codebook design constructs the first codeword representing the whole long-term channel correlation in the plane with the Kronecker product of two DFT matrices generated for two orthogonal ULAs. We proved the validity of this construction theoretically, and verified that the proposed codebook outperforms other kinds of codebooks in terms of the channel coverage and the achievable sum rate under various scenarios via simulations. The proposed codebook design can contribute to precoding solutions for large-scale array antenna technologies, which would be probably applied to future Beyond 4 G systems. Our future work will consider advanced multiuser scheduling algorithms as well as robust receiving algorithms for massive MIMO.

Acknowledgments

References

[1] F. Rusek, D. Persson, B. K. Lau et al., "Scaling up MIMO: opportunities and challenges with very large arrays," *IEEE Signal Processing Magazine*, vol. 30, no. 1, pp. 40–60, 2013.

[2] E. Visotsky and U. Madhow, "Space-time transmit precoding with imperfect feedback," *IEEE Transactions on Information Theory*, vol. 47, no. 6, pp. 2632–2639, 2001.

[3] T. Inoue and R. W. Heath Jr., "Kerdock codes for limited feedback precoded MIMO systems," *IEEE Transactions on Signal Processing*, vol. 57, no. 9, pp. 3711–3716, 2009.

[4] J. C. Roh and B. D. Rao, "Design and analysis of MIMO spatial multiplexing systems with quantized feedback," *IEEE Transactions on Signal Processing*, vol. 54, no. 8, pp. 2874–2886, 2006.

[5] D. J. Love and R. W. Heath Jr., "Limited feedback unitary precoding for spatial multiplexing systems," *IEEE Transactions on Information Theory*, vol. 51, no. 8, pp. 2967–2976, 2005.

[6] K. Schober, R. Wichman, and T. Koivisto, "MIMO adaptive codebook for closely spaced antenna arrays," in *Proceedings of the European Signal Processing Conference (EUSIPCO '11)*, pp. 1–5, Barcelona, Spain, August 2011.

[7] D. J. Ryan, I. V. L. Clarkson, I. B. Collings, D. Guo, and M. L. Honig, "QAM codebooks for low-complexity limited feedback MIMO beamforming," in *Proceedings of the IEEE International Conference on Communications (ICC '07)*, pp. 4162–4167, June 2007.

[8] A. L. Moustakas, H. U. Baranger, L. Balents, A. M. Sengupta, and S. H. Simon, "Communication through a diffusive medium: coherence and capacity," *Science*, vol. 287, no. 5451, pp. 287–290, 2000.

[9] T. Shuang, T. Koivisto, H.-L. Määttänen, K. Pietikäinen, T. Roman, and M. Enescu, "Design and evaluation of LTE-Advanced double codebook," in *Proceedings of the IEEE 73rd Vehicular Technology Conference (VTC '11)*, pp. 1–5, Yokohama, Japan, May 2011.

[10] A. M. Sayeed, "Deconstructing multiantenna fading channels," *IEEE Transactions on Signal Processing*, vol. 50, no. 10, pp. 2563–2579, 2002.

[11] K. Amiri, D. Shamsi, B. Aazhang, and J. R. Cavallaro, "Adaptive codebook for beamforming in limited feedback MIMO systems," in *Proceedings of the 42nd Annual Conference on Information Sciences and Systems (CISS '08)*, pp. 994–998, March 2008.

[12] G. Levin and S. Loyka, "On capacity-maximizing angular densities of multipath in MIMO channels," in *Proceedings of the 72nd Vehicular Technology Conference Fall (VTC '10)*, Ottawa, Canada, September 2010.

[13] C. F. V. Loan, "The ubiquitous Kronecker product," *Journal of Computational and Applied Mathematics*, vol. 123, no. 1-2, pp. 85–100, 2000.

[14] A. Paulraj, R. Nabar, and D. Gore, *Introduction To Space-Time Wireless Communications*, Cambridge University Press, Cambridge, UK, 2003.

[15] X. Gao, O. Edfors, F. Rusek, and F. Tufvesson, "Linear precoding performance in measured very-large MIMO channels," in *Proceedings of the 74th Vehicular Technology Conference (VTC '11)*, San Francisco, Calif, USA, September 2011.

[16] Rec. ITU-R M. 1225, guidelines for evaluation of radio transmission technologies for IMT-2000, 1998.

[17] J. C. Roh and B. D. Rao, "Design and analysis of MIMO spatial multiplexing systems with quantized feedback," *IEEE Transactions on Signal Processing*, vol. 54, no. 8, pp. 2874–2886, 2006.

[18] "IST-WINNER II Deliverable 1. 1. 2 v. 1. 2. WINNER II Channel Models, IST-WINNER2," Tech. Rep., 2007, http://www.ist-winner.org/deliverables.html.

[19] "Evolved Universal Terrestrial Radio Access (E-UTRA), Physical layer procedures," 3GPP TS 36. 213 V10. 6. 0, 2012.

[20] E. Jorswieck, A. Sezgin, B. Ottersten, and A. Paulraj, "Feedback reduction in uplink MIMO OFDM systems by chunk optimization," *Eurasip Journal on Advances in Signal Processing*, vol. 2008, Article ID 597072, pp. 1–14, 2008.

Journal of
Engineering

The Scientific
World Journal

International Journal of
Rotating
Machinery

Journal of
Sensors

International Journal of
Distributed
Sensor Networks

Advances in
Civil Engineering

Journal of
Control Science
and Engineering

Journal of
Robotics

Journal of
Electrical and Computer
Engineering

Hindawi

Submit your manuscripts at
http://www.hindawi.com

Advances in
OptoElectronics

VLSI Design

International Journal of
Navigation and
Observation

Modelling &
Simulation
in Engineering

International Journal of
Aerospace
Engineering

International Journal of
Chemical Engineering

International Journal of
Antennas and
Propagation

Active and Passive
Electronic Components

Shock and Vibration

Advances in
Acoustics and Vibration